

EFFECT OF COMPACTING PRESSURE ON MICROSTRUCTURE, PHYSICAL AND MECHANICAL PROPERTIES OF NiTi SMA PREPARED BY POWDER METALLURGY

Noora Mohammed Gased ,Haydar Al-Ethari, Ali Hubi Haleem

Department of Metallurgical Engineering, College of Materials Engineering, Babylon
University, Babylon, Iraq

ABSTRACT

This study investigates the effect of different compacting pressures on microstructure, physical and mechanical properties of NiTi shape memory alloys. The samples were prepared by powder metallurgy technique. The powder mixture containing 55wt% Ni and 45wt% Ti were mixed for 5 hours, compacted at different pressures (400, 600, 800 and 900) MPa to cylindrical samples, and sintered in two stages. First heating the compacted samples at temperature of 450°C for 2 hours and at a temperature of 950°C for 6 hours under vacuum conditions (10^{-4} torr). The XRD test shows that the sample compacted at 800 MPa are consisting of three phases (NiTi monoclinic phase, NiTi cubic phase, Ni₃Ti hexagonal phase). From the results, it was found that compacting pressure has essential effect on; improvement of shape memory effect properties (1.30-5.60)%, increasing hardness (from 80.4 to 137) and compressive strength (from 127.43 to 431.04) MPa and decrease porosity percentage (from 32 to 22)%.

Key words: SMA, NiTi, Nitinol, powder metallurgy, compacting pressure.

تأثير ضغط الكبس على التركيب المجهرى والخواص الميكانيكية والفيزيائية لسبيكة نيكل تيتانيوم ذاكرة الشكل المحضرة بطريقة ميتالورجيا المساحيق

نورا محمد كاسد، د. حيدر عبد الحسن العذارى، د. علي هوبي حليم

الخلاصة:

يتضمن هذا العمل دراسة تأثير ضغوط الكبس على التركيب المجهرى والخواص الفيزيائية والميكانيكية لسبيكة نيكل تيتانيوم ذاكرة الشكل. تم تحضير العينات باستخدام طريقة تكنولوجيا المساحيق، يتألف خليط المساحيق من (45wt.% Ti + 55wt.% Ni). خلطت المساحيق الأساسية لمدة 5 ساعات ثم كبست بتسليط ضغوط مختلفة مقدارها (400, 600, 800 and 900 MPa) لتتحول الى نماذج أسطوانية الشكل. تمت عملية التلبيد بمرحلتين، أولاً سخنت بدرجة حرارة 450 درجة سيليزية لمدة ساعتين ومن ثم استمرت الى درجة حرارة 950 درجة سيليزية ولمدة 6 ساعات في جو مفرغ من الهواء لغاية (10^{-4} torr). اوضح اختبار حيود الاشعة السينية بان النماذج الملبدة والمكبوسة بضغط 800 MPa تحتوي

على ثلاثة أطوار (طور الأوستنايت NiTi وطور المارتنسايت NiTi إضافة إلى طور Ni₃Ti). من خلال النتائج وجد أن ضغط الكبس يؤثر بشكل أساسي على تحسين خواص استعادة الذاكرة وزيادة الصلادة ومقاومة الانضغاط وتقليل نسبة المسامية.

1. INTRODUCTION

Shape memory alloys (SMA) possess different properties compared to conventional metals. This type of alloy is capable of remembering its shape following a deformation. Relatively large recoverable strain of around 8% is one of the SMA's distinct properties, which makes it a favorable candidate for applications involving large deforming loads. Nitinol (NiTi alloy) is one of the most well-known shape memory alloys. Such alloy is composed of nickel and titanium in approximately equiatomic ratio [1].

Nitinol is capable of displaying pseudoelasticity giving the material the ability to transform between phases upon loading and unloading and recover to its original zero strain shape after significant deformation. With the properties such as repeatability, wear resistance, corrosion resistance and biocompatibility, NiTi is the most commercially successful SMA [2]. The shape memory and pseudoelastic characteristics coupled with the biocompatibility of NiTi alloys make them an attractive candidate for medical applications such as cardiovascular and orthopedic applications [3]. Furthermore, several studies such as Sadrnezhaad, et.al. [4] reported that commercially pure nickel-titanium powders were compacted and sintered at different temperatures for different times. Amorphization and interatomic phase formation were determined by X-ray diffractometry, scanning electron microscopy and differential scanning calorimetry. Porosity, virtual density, transition temperatures and the amount of Ni₃Ti first increased and then decreased with the milling time. Carlton G. Slough, et.al. [5] studied the nitinol shape-memory alloy solid-solid transition using differential scanning calorimetry (DSC), which reveals the reversible and hysteretic nature of this transition. The results show that the DSC is an excellent technique for examining the solid-solid transition in nitinol shape-memory alloys. This transition is a first order transition that shows no dependency on heating rate. This research aims at investigating the effect of compacting pressure (400 to 900) MPa on mechanical properties of Ni-Ti shape memory alloys prepared by powder metallurgy.

2. EXPERIMENTAL PART

In order to prepare samples of NiTi SMAs, powder metallurgy technique had been used. This method involves weighting the powders (55wt%Ni with 45wt%Ti) by using a sensitive balance device, mixing, compacting and then sintering them. The purity, average particle size and the original of ingredients used in this work are shown in **Table 1**.

Wet mixing was carried out by the electrical rolling mixer apparatus to achieve a homogenous distribution of the powders. Stainless steel balls with different diameters had been used during the mixing process to ensure refining and mixing the powders for a period of 5 hours. After mixing, all samples were compacted at 400, 600, 800 and 900 MPa. Compacting was achieved on an electric hydraulic press machine. A steel die of 10 mm in diameter was used to prepare samples of 10mm in diameter and 5mm in height. Following the compaction, all samples were sintered at two stages, the first at 450 °C for 2hrs and then heated at 950 °C for 6hrs (the samples were allowed to heat up with a heating rate of 10°C/min) using a vacuum furnace (GSL-1600x). The pressure of the vacuum furnace was 10⁻⁴ torr.

3. TEST

3.1. Particle Size Measurement

The particle size for Ni and Ti powders was tested by using laser particle size analyzer [model: better size 2000].

3.2. Microstructure

All surfaces of the samples including the edges were wet ground using 120, 220, 320, 600, 1000, 1200 and 2000, grit silicon carbide papers. Etching solution consisting of [10% of HF, 20% of HNO₃ and 70% of H₂O] at room temperature was used[6]. The samples was washed with distilled water and dried using electric drier. Optical microscope and Scanning Electron Microscope (SEM) were used to capture the microstructure of the surface sample.

3.3. X-Ray Diffraction Analysis

X-Ray diffraction method was used to define the phases of sintered samples and the green compact samples in order to compare these diffraction patterns with sintered diffraction patterns for the same samples. The X - ray generator with Cu at 40 KV and 30 mA was used. The X- ray is operating at a scanning speed of 7° (2θ) per minute. The detector was moved through an angle of 2θ = 20 to 80 degrees.

3.4. Density and Porosity Measurement

The green density of compacted samples was calculated as follows[7]:

$$\rho_g = \frac{m_g}{V_g} \dots\dots\dots\text{Eq.1}$$

where : ρ_g: green density (g/cm³)

m_g : green mass of the compacted sample(g); and V_g = volume of the compact (cm³).

The ratio of pore volume to the total volume is called green porosity which can be determined from the following equation[7]:

$$P_g = (1 - \rho_g / \rho_{th}) \times 100 \dots\dots\dots\text{Eq.2}$$

Where P_g - green porosity percentage%

ρ_g : Green density of the green sample (g/cm³)

ρ_{th}: theoretical density of the bulk material (g/cm³) .

The theoretical density(ρ_{th}) can be calculated by the weight percentages of elemental powder multiplies by its theoretical density as follows[8] .

$$\rho_{iB} = \sum_{i=1}^n Wt_i * \rho_i + Wt_2 * \rho_2 + Wt_3 * \rho_3 + \dots\dots\dots + Wt_n * \rho_n \dots\dots\text{Eq.3}$$

Where:

P_{1,2,...,n}: theoretical density of the elemental powder (g/cm³)

Wt_{1,2,...,n} : weight percentage (%)of elemental powder in the alloy.

The density and porosity of sintered specimens are calculated basing on ASTM B-328 [9]following the procedure of:

- The specimen was dried at 100°C for 6 hour in vacuum furnace under a pressure of ((10⁻⁴ torr) then cooled to room temperature, the weight of dry specimen was recorded as mass A.
- At room temperature, the specimen was immersed in oil (with a density D_o = 0.8 g / cm³) by using a suitable evacuating pump for 30 min.
- Weighing the fully impregnated specimen in air, the mass was recorded as B.
- Weighing the fully impregnated specimen in water (mass,F).
- Measuring the temperature and find the density of water at this temperature. For this study, the temperature was 30°C, at which the density of water (D_w) at this temperature was 0.9956 g / cm³.The density (D) was computed according to the following equation:

$$D = [(A/B - F)] D_w \dots\dots\dots \text{Eq.4}$$

and the porosity was measured as:

$$P = \left[\frac{B - A}{(B - F) D_o} \times 100 \right] D_w \dots\dots\dots \text{Eq.5}$$

3.5. Hardness Test

Macro hardness Brinells tester was used to measure the hardness of the sintered samples with 2.5mm ball diameter as indentation ball and (31.25N) as applied load .An average of three readings had been recorded in this test.

3.6. Compression Test

The compression test was performed according to ASTM B925-08 specifications via universal testing machine type (WDW 200,china). Standard sintered sample of (10mm diameter × 12mm height) were used .The test was achieved at constant loading speed of 0.1mm/min.

3.7. Shape Memory Effect

The Shape memory effect was determined basing on Brinell indentation as follows[10]:

$$\text{Shape memory effect (SME \%)} = \frac{d_b - d_a}{d_b} \times 100 \dots\dots\dots \text{Eq.6}$$

Where:

d_b = average impression diameter in (μm) before heating to 80°C.

d_a = average impression diameter in (μm) after heating to 80°C.

4. RESULTS AND DISCUSSION

4.1. Particle Size Analysis

Particle size analysis results of Ni and Ti powders are shown in **Figures (1) and (2)** respectively. It is clear that the average size of the powder was 12.08 μm for Ti and 36.80 μm for Ni respectively.

4.2. Green Density and Porosity of Compacts

The effect of compacting pressure on green density and green porosity of the prepared samples is shown in **Figure(3)**.As it is clear an increase in the compacting pressures resulted in an increase in the green density and decrease in the green porosity of the prepared samples. The maximum green density attained was 5.23 (g/cm^3), corresponding to a porosity level of 25% due to maximum compacting pressure of 900 MPa. Increasing in pressure causes the elimination of more pores and creation of new contacts, and finally homogeneous deformation of the whole compact[11].

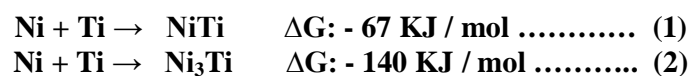
4.3. Density and Porosity after Sintering

The effect of compacting pressure on the density of the sintered sample is shown in **Figure(4a)**.The results indicate that the density after sintering is increased with the compacting pressure. This increase is likely due to the shrinkage of original pores during sintering.

Figure(4b) shows the change of final porosity with compacting pressure. It is found that porosities are decreased after sintering, this reduction is attributed to the high temperature during sintering which led to reduce the size of pores in the structure and rejected the air from the pores.

4.4. X-Ray Diffraction Analysis

The XRD pattern of the green compact sample is shown in **Fig.(5)**. It can be seen that only Ni and Ti phases were detected because during compacting process, no phase transformation take place. **Figure (6)** represents the chart of x-ray diffraction results after sintering process of the alloy sample prepared using a compacting pressure of 800 MPa. The full transforming of NiTi alloy to monoclinic NiTi phase ,cubic NiTi phase and hexagonal Ni_3Ti phase can be easily observed. The suggested reactions during the process are as following [12].



According to the phase diagram of NiTi system , NiTi and Ni_3Ti are stable compounds, also reaction according to equ.2 is more thermodynamically favored than that represented by eq.1. Consequently, it is difficult to remove the Ni_3Ti from sintered sample only by altering the sintering condition[12,13].

4.5. Microstructure Observation of the Sintered Samples

Figure(7) shows the microstructure of all sintered samples compacted at different pressures. The microstructure of these alloys showed pores with different size, present phase and grain boundaries. The pores are rarely interconnected and randomly distributed. It can be observed that with increasing compacting pressure from (400 to 900) MPa ,the pores become smaller, the

pore number decrease and its distribution becomes more uniform. This is because when compacting pressure increased the pore tend to be compact and take around.

All scanning electron microscope (SEM) images of the etched samples with different compacting pressure are shown in **Figure(8)**, respectively. SEM images are sensitive to chemical composition as result the microstructure of sintered samples showed two kinds of phases (NiTi and Ni₃Ti).The formation of martensite phase from disorder or ordered B2 (austenite) in the sintered sample is clearly. The martensite phase formed in all alloys have a needle shaped grains, because the diffusion less feature of martensite transformation.

4.6. Hardness Test

Figure (9) demonstrates the hardness of the specimens compacted at different pressures after the sintering process. The results indicate the increase in hardness of the specimens with increasing the compacting pressure. This agreed with the fact that as the compacting pressure is increased, the bonding between the particles is better (i.e. better inter diffusion) which in term leads to more pores elimination[14].

4.7. Compression Test

Table (2) shows the values of compressive strength (σ_{com}), are increased with increasing the compacting pressure because the total amount of porosity in the mass are decreased. The results are in agreement with ref.[10].

4.8. Shape Memory Effect

The SME values as a function of compacting pressure (400,600,800 and 900MPa) for all prepared alloy samples are shown in figure(10). It is clear from this figure that the SME increased by the increasing of the compacting pressure due to the elimination of porosity. SME values for master alloys showed smaller values than the values of dense form which reach to 8-10 % [3].

5. CONCLUSIONS

Based on the results obtained in the present work, the conclusions can be summarized as follows:

- 1- Scanning electron microscope observation indicated that the most samples compacted at (400 to 900) MPa have a clear martensitic structure.
- 2- The increasing in compacting pressure from (400 to 900) MPa for master NiTi alloys resulted in an improvement in shape memory effect (SME) and hardness, increasing in density and decreasing in porosity.
3. Compressive strength of NiTi SMA alloys produced by PM increases with decreasing the porosity (increasing compacting pressure).

6. REFERENCES

1. Z. Karbaschi, " **Torsional Behavior of Nitinol: Modeling and Experimental Evaluation**" M.Sc. thesis, University of Toledo, 2012.
2. L. Tan and W. C. Cron, " **In Situ TEM Observation of Two - Step Martensitic Transformation in Aged NiTi Shape Memory Alloy**" Scripta material, Vol. 50, 2004, PP. 819 – 823.
3. C. Dimitis and Lagoudas, " **Shape Memory Alloys Modeling and Engineering Application** ", Texas A&M University, USA, 2008.
4. S. K. Sadrnezhaad and A. R. Selahi, " **Effect of Mechanical Alloying and Sintering on Ni-Ti Powders**", Materials and Manufacturing Processes, Vol.19, 2004, PP.475-486.45-
5. Carlton G. Slough, " **A Study of the Nitinol Solid-Solid Transition by DSC**", 2007.
6. J. Jafari, S. Zebarjad and S. Sajjadi, " **Effect of pre - strain on microstructure of Ni - Ti orthodontic arch wires** ", Materials Science and engineering A. 473 , 2008 , pp . 42 - 48.
7. R. Khalifehzadeh, S. Forouzan, H. Arami and S.K. Sadrnezhaad, " **Prediction of The Effect of Vacuum Sintering Conditions on Porosity and Hardness of Porous NiTi Shape Memory Alloy using ANFIS**", Computational Materials Science ,Vol.40 ,2007,PP. 359–365.
8. S.M.Jawad, " **Effect of Cr and Cr Additives On Corrosion and Dry Sliding Wear of NiTi Shape Memory Alloy**", M.Sc. thesis Department of Metallurgical Engineering, University of Babylon,2015.
9. ASTM B - 328 " **Standard Test Method for Density , Oil Content , and Interconnected Porosity of Sintered Metal Structural Parts and Oil - Impregnated Bearing** ", ASTM International, 2003.
10. N.M.Dawood, " **Preparation and Characterization of Bio Nitinol With Addition of Copper**", PhD. thesis, Materials Engineering Department ,University of Technology/ Iraq,2014.
11. T. Aydogmus and A. S. BOR, " **Production and Characterization of Porous TiNi Shape Memory Alloys**", Turkish J. Eng. Env. Sci.,Vol.35 ,2011 ,PP.69-82.
12. S.L.Zhu, X.J.Yang, D.H.Fu, L.Y.Zhang ,C.Y.Li and Z.D.Cui, " **Stress-Strain Behavior of Porous NiTi Alloys Prepared by Powder Sintering**" Materials Science and Engineering A408,2005,pp.264-268.
13. Bing-Yun Li , Li-Jian Rong , Yi-Yi Li and V. E. Gjunter , " **An Investigation of The Synthesis of Ti-50 At. Pct Ni Alloys Through Combustion Synthesis and Conventional Powder Sintering**", Metallurgical and Materials Transactions A, Vol..31A, Issue 7,July 2000,PP.1867-1871.
14. Sheelan R. Areef, " **Characterization of Ni-Ti Shape Memory Alloys**", Eng. & Tech. Journal, Vol. 28, No.5 , 2010.

Table (1): Powders used to prepare samples of NiTi alloy.

Materials	Purity %	Average Particle Size(μm)	Source
Nickel Powder	99.75%	12.08	Changxing Galaxy International Trade Co.,LTD.
Titanium Powder	99.65%	36.80	

Table (2): Compressive strength for all samples compacted at different pressure.

Sample with different compacting pressure	400MPa	600MPa	800MPa	900MPa
Compressive strength (σ_{com})MPa	127.43	221.15	338.58	431.04

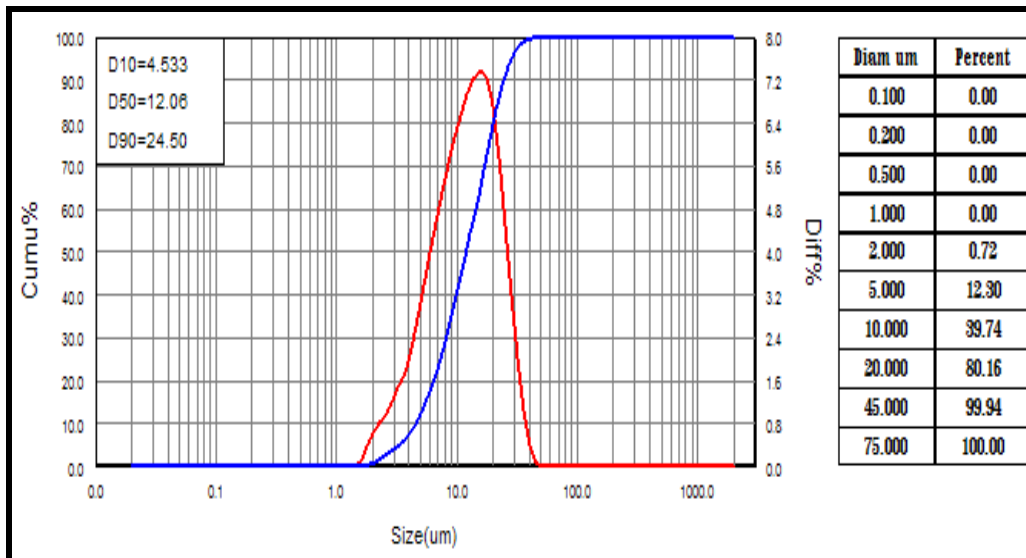


Figure (1): Particle size distribution of Ti powder used in this study.

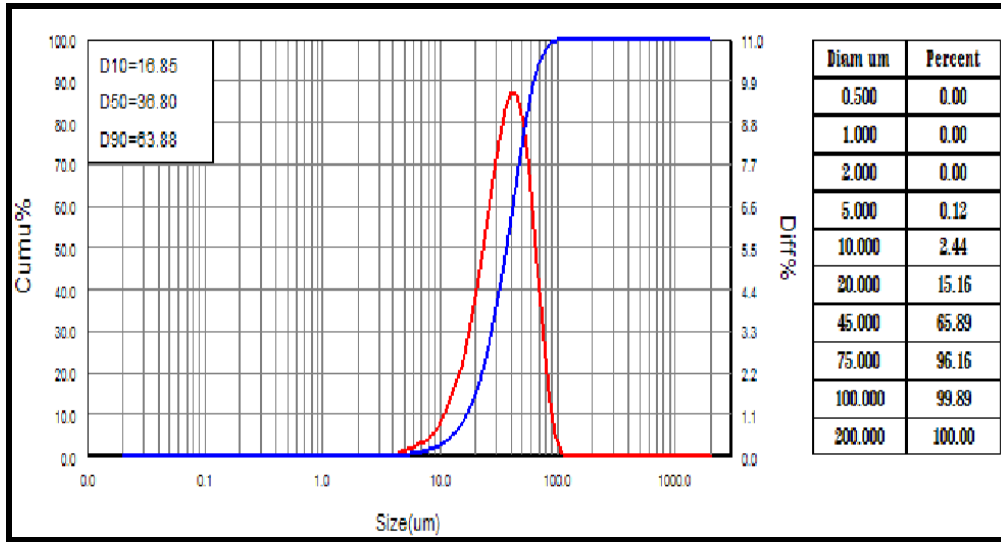
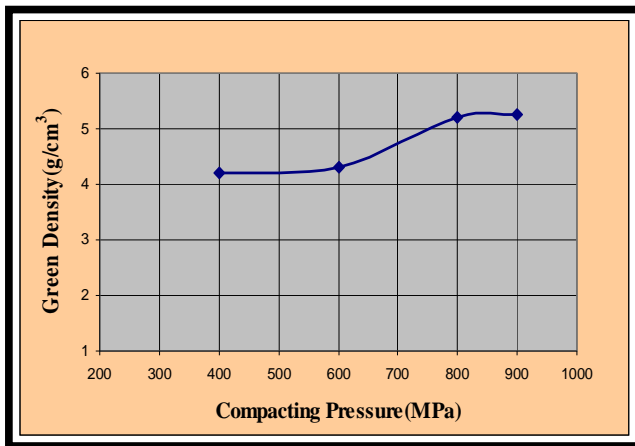
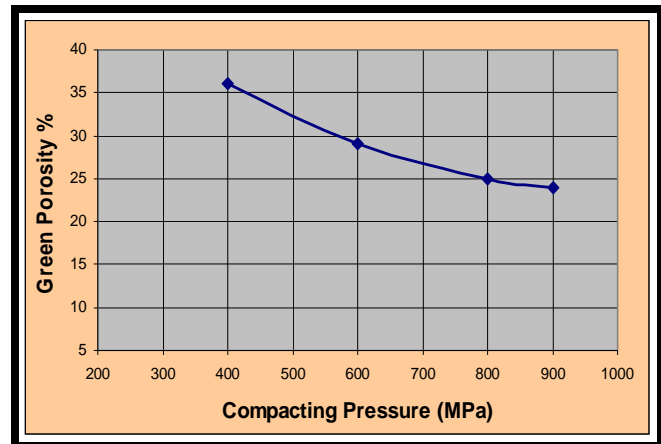


Figure (2): Particle size distribution of Ni powder used in this study.

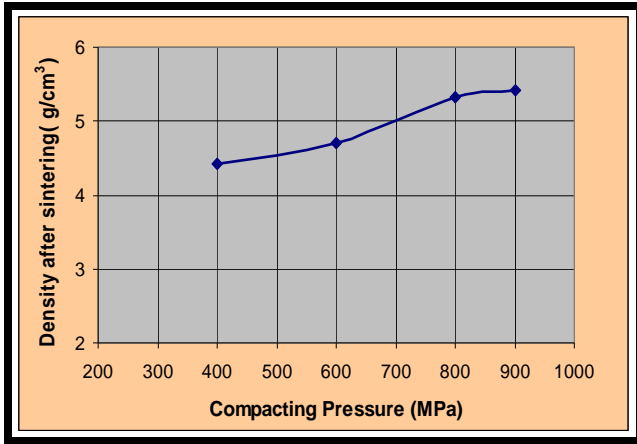


(a)

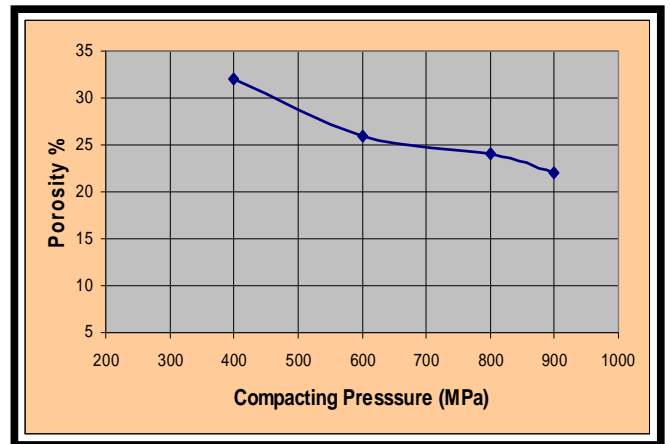


(b)

Fig. (3) Effect of compacting pressure on:(a) Green density of the prepared sample, (b) Green porosity of the prepared sample.



(a)



(b)

Fig. (4) Effect of compacting pressure on :(a) density of the sintered samples,(b) porosity of the sintered samples.

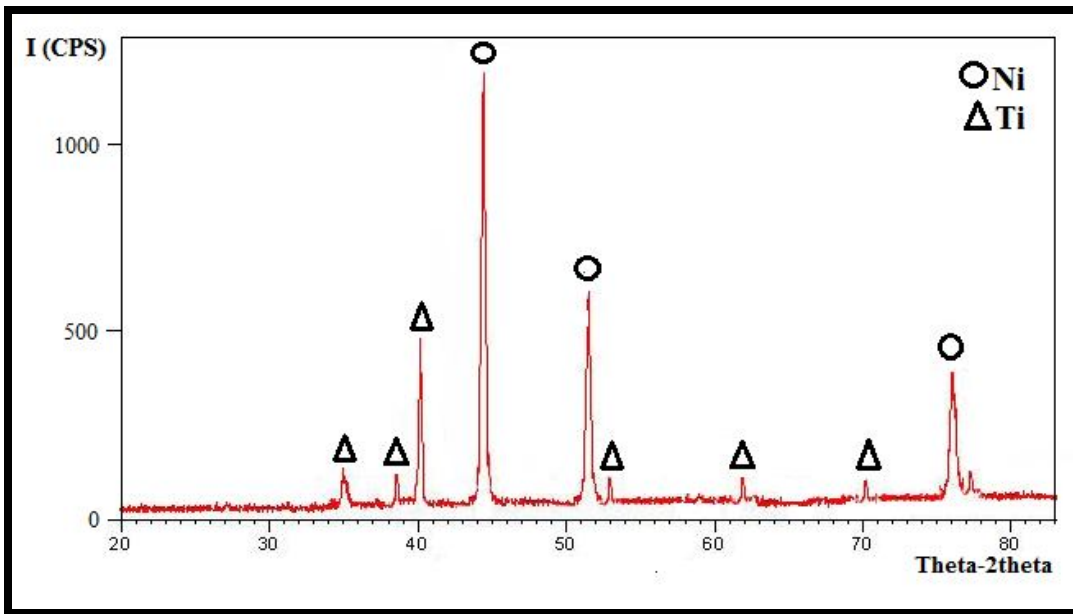


Fig.(5) XRD pattern of the green compact sample.

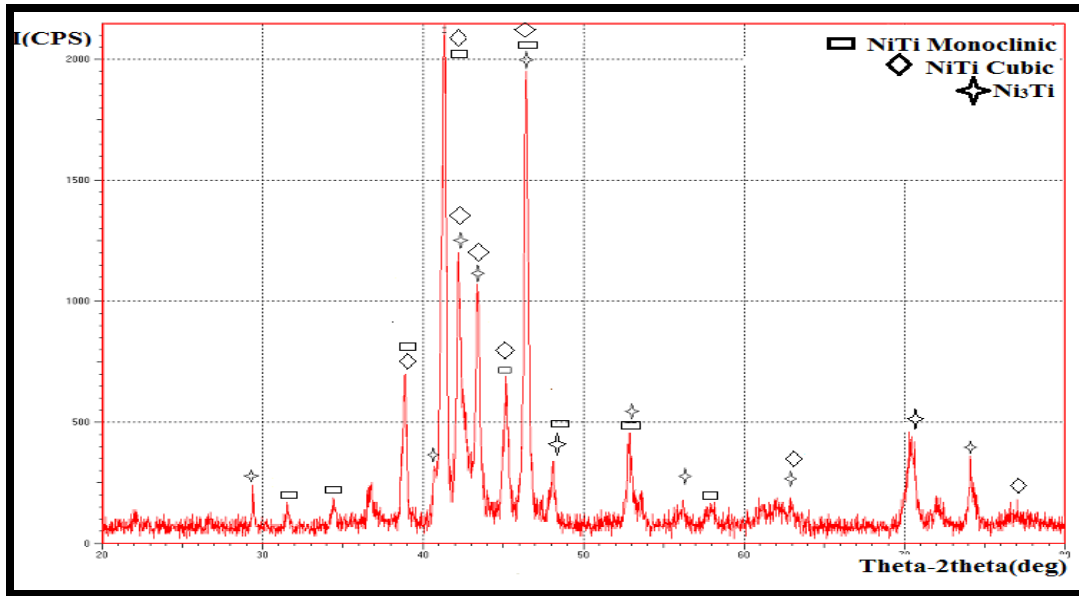


Fig.(6) XRD pattern of sample compacted at 800 pressure after sintering.

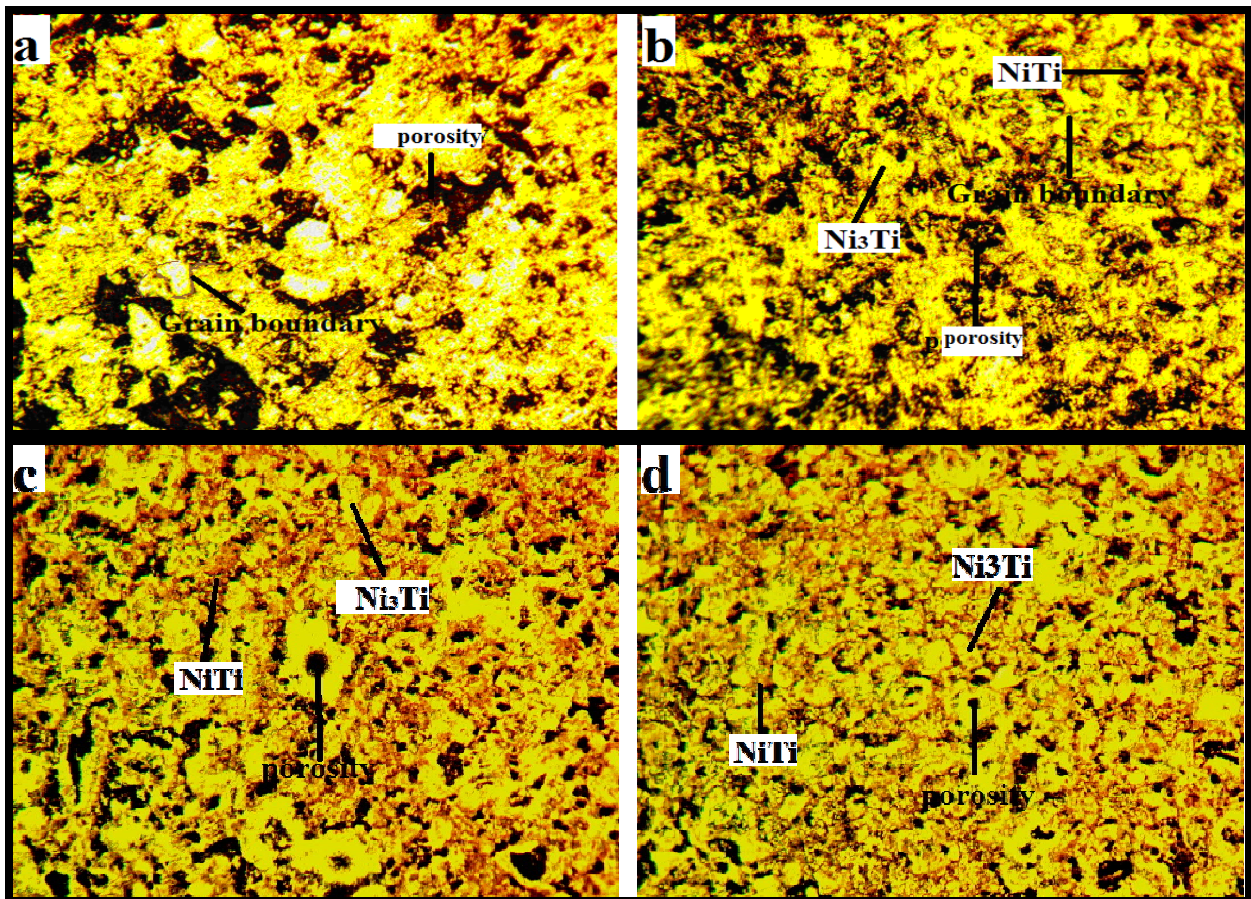
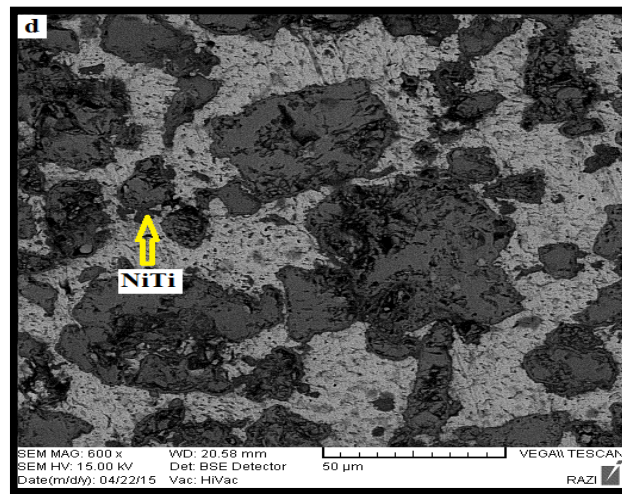
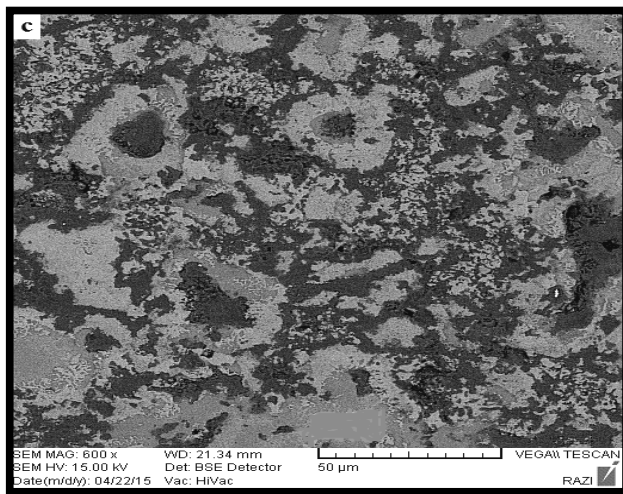
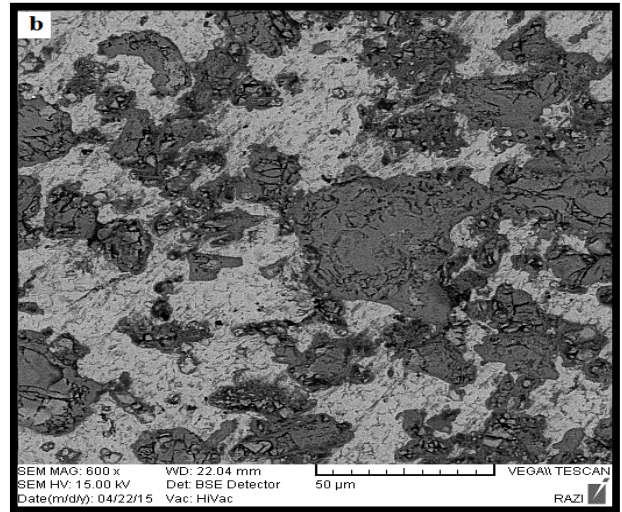
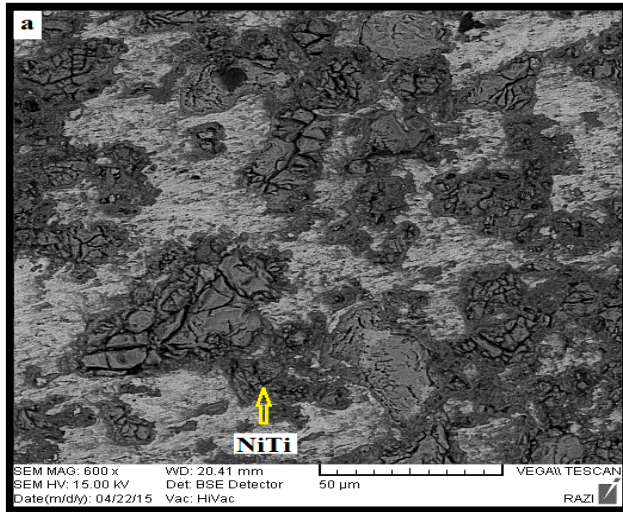


Fig. (7) Microstructure for alloys compacted at a: 400 MPa b: 600 MPa c: 800 MPa and d: 900 MPa respectively(400x).



**Fig.(8) SEM images for etched alloys compacted at a: 400 MPa b: 600 MPa
c: 800 MPa d: 900MPa.**

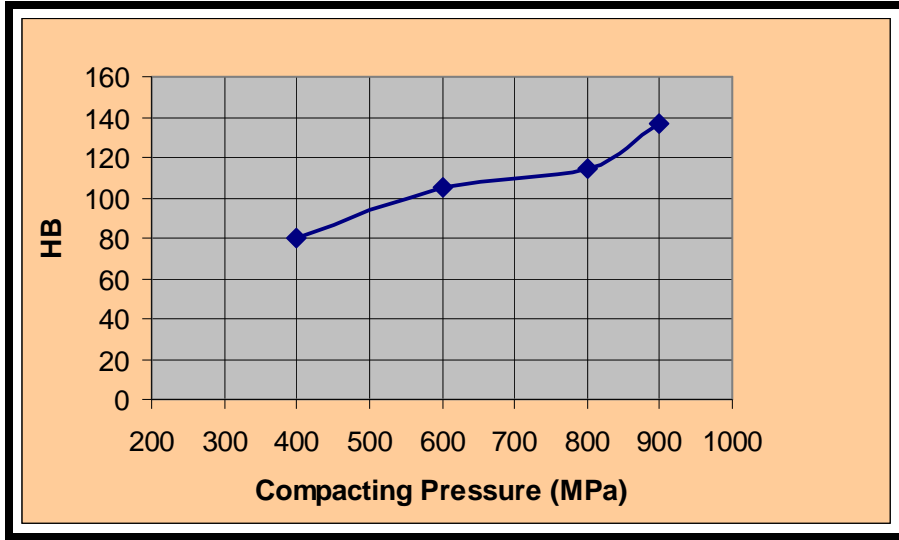


Fig.(4.13) Effect of compacting pressure on the HB values of the sintered alloy sample.

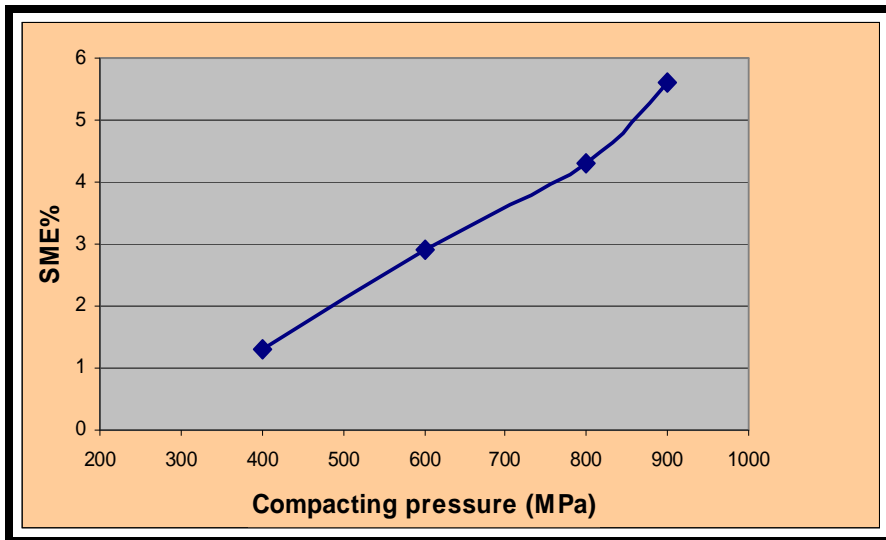


Fig. (10) Effect of compacting pressure on SME properties obtained from Brinell Hardness test.